Agricultural and Forest Meteorology 271 (2019) 83–91

Contents lists available at ScienceDirect

Agricultural and Forest Meteorology

journal homepage: www.elsevier.com/locate/agrformet

Precipitation has dominant influences on the variation of plant hydraulics of the native *Castanopsis fargesii* (Fagaceae) in subtropical China

Xingyun Liang[a,1], Pengcheng He[a,b,1], Hui Liu[a], Shidan Zhu[c], Isaac Kazuo Uyehara[d], Hao Hou[a,b], Guilin Wu[a], Hui Zhang[a], Zhangtian You[a,b], Yiying Xiao[a,e], Qing Ye[a,*]

[a] Key Laboratory of Vegetation Restoration and Management of Degraded Ecosystems, and Guangdong Provincial Key Laboratory of Applied Botany, South China Botanical Garden, Chinese Academy of Sciences, Xingke Road 723, Guangzhou 510650, China
[b] College of Resources and Environment, University of Chinese Academy of Sciences, Yuquan road 19A, Beijing 100049, China
[c] Guangxi Key Laboratory of Forest Ecology and Conservation, College of Forestry, Guangxi University, Nanning 530004, China
[d] Department of Ecology and Evolutionary Biology, Princeton University, 106A Guyot Hall, Princeton, NJ, 08540, USA
[e] College of Natural Resources and Environment, South China Agricultural University, Wushan Road 483, Guangzhou 510642, China

ARTICLE INFO

Keywords:
Hydraulic architecture
Intraspecific phylogeny
Intraspecific variation
Precipitation gradient
Climate change

ABSTRACT

Understanding the roles of climate and intraspecific phylogeny in affecting the variation of plant hydraulics can provide insights into species distribution in different habitats. In the present study, we quantified ten functional traits characterizing branch and leaf hydraulic architecture of *Castanopsis fargesii* from 12 populations along a precipitation gradient (1120–1690 mm y^{-1}), covering an 1800-km-long west-center-east transect in the subtropical region of China. We also conducted phylogenetic analyses to test the role of intraspecific phylogeny in affecting the variation of hydraulic architecture. We found that, with decreasing precipitation, branch vessel density remained unchanged while hydraulically weighted vessel diameter (D_h) declined by 31.9%, leading to a 74.3% reduction in theoretical hydraulic conductance (K_{th}). In parallel, leaf vein density (VD) and stomatal pore area index (SPI) declined by 14.6% and 29.9%, respectively. Leaf turgor loss point also declined significantly from −1.51 to −2.29 MPa along the precipitation gradient. In addition, functional traits related to hydraulic efficiency (i.e. K_{th}, D_h, VD and SPI) were positively correlated, whereas both trait variation and trait-trait correlations were not significantly affected by intraspecific phylogeny, as indicated by the values of Blomberg's $K < 1$ and the consistency between principle component analysis and phylogenetic principle component analysis. We conclude that, hydraulic architectures of branch and leaf in *C. fargesii* varied remarkably under the primary influence of precipitation, suggesting that this subtropical tree species has a high degree of plasticity in terms of hydraulic adjustment, allowing it to cope with shifts in precipitation under future climate change.

1. Introduction

Hydraulic architecture plays a critical role in water transport and consequently affects the growth, survival and distribution of trees under different environment conditions. For angiosperm trees that demand relatively large amounts of water for gas exchange and growth, a network composed of wide vessels (Sperry et al., 2006; Hacke et al., 2017), high leaf vein density (Brodribb et al., 2007) and large stomatal pore area (Sack et al., 2003) is expected. However, wider vessels tend to have more inter-vessel pits and thus greater probabilities for air-seeding to proceed (Wheeler et al., 2005; Hacke et al., 2006; Christman et al., 2009), thus be more vulnerable to embolism (Cai and Tyree, 2010; Hacke et al., 2017), which impairs water transport and may lead to tree mortality (McDowell et al., 2008; Anderegg et al., 2016; Choat et al., 2018). By contrast, narrow vessels and dense sapwood are generally associated with high resistance to embolism, but at the cost of hydraulic conductance (Hacke et al., 2001; Jacobsen et al., 2007). Furthermore, the structure of pits (such as the porosity and thickness of pit membranes and the size of pit aperture) also determines both hydraulic efficiency and safety (Choat et al., 2008; Jansen et al., 2009). All the physical constraints lead to a hydraulic efficiency-safety trade-off (Hacke and Sperry, 2001), which is supported, thought weakly, by many empirical studies across species (Maherali et al., 2004; Gleason et al., 2015). Therefore, we might also expect a hydraulic efficiency-safety trade-off within species and an adaptation of hydraulic architecture to different water availabilities.

* Corresponding author.
E-mail address: qye@scbg.ac.cn (Q. Ye).
[1] These two authors contributed equally to this work.

https://doi.org/10.1016/j.agrformet.2019.02.043
Received 7 September 2018; Received in revised form 6 February 2019; Accepted 28 February 2019
Available online 06 March 2019

Modification of branch and leaf hydraulic architecture across environments has been widely documented, but mostly at the interspecific level (Pfautsch et al., 2016; Blonder et al., 2017; Larter et al., 2017; Schneider et al., 2018; Zhu et al., 2018), while only a few studies have investigated the intraspecific variation in hydraulic architecture across precipitation gradients at the branch level, and even fewer at the leaf level (Martínez-Vilalta et al., 2009; Schreiber et al., 2015; Schuldt et al., 2016). Therefore, for a better understanding and predicting tree responses to climate change, it is essential to investigate intraspecific variation in hydraulic architecture across climates such as the gradient of precipitation.

Intraspecific variation in hydraulic architecture can be contributed by phenotypic plasticity, the ability of a single genotype to produce different phenotypes when exposed to different environmental conditions, and/or by genotypic differences that is caused by intraspecific phylogeny (Schreiber et al., 2015; Ramírez-Valiente et al., 2018). Comparative phylogenetic analyses could statistically test to what extent trait variation among populations is consistent with the assumption that closely related populations tend to have more similar traits than distantly related populations (Blomberg et al., 2003; Wiens et al., 2010). The phylogenetic analyses have been broadly used to study intraspecific trait variation in both animals (Wiens et al., 1999; Niewiarowski et al., 2004; Olave et al., 2017) and plants such as evergreen broad-leaved trees (Ramírez-Valiente et al., 2018; Rungwattana et al., 2018), using methods such as the Blomberg's *K*-statistic (Blomberg et al., 2003). When the Blomberg's *K* is smaller than 1, intraspecific variation in traits would not be mainly driven by intraspecific phylogeny, but instead by phenotypic plasticity (Blomberg et al., 2003).

The evergreen broad-leaved forests (EBLFs) in subtropical China, which occur between 24–32 °N and 99–123 °E and cover about 25% of China's land area, play a critical role in biodiversity and the global carbon budget (Song, 1988; Wang et al., 2007), with the annual rainfall ranging from 900 to 1200 mm in the semi-moist west to 1000–2000 mm in the moist east regions (Wang et al., 2007). In the past decades, soil moisture in subtropical China has decreased significantly due to changes in precipitation pattern, with more rain-free days and severe extreme hydrological events per year, leading to the frequent occurrences of droughts and floods (Zhou et al., 2011). Changes in water availability have already caused shifts in the tree species composition of EBLFs (Zhou et al., 2013; Li et al., 2015b), calling for an urgent need to assess hydraulic responses of EBLFs tree species to changes in water availability.

Castanopsis fargesii (Fagaceae) is a dominant tree species of EBLFs, covering a wide range about 1800-km-long from west to east in subtropical China (Sun et al., 2014). Recently, the intraspecific phylogenetic relationships among different *C. fargesii* populations were constructed (Sun et al., 2014). It has also been shown that, *C. fargesii* populations possess a high degree of genetic diversity, and frequencies of some alleles are strongly correlated with precipitation (Li et al., 2014). However, if hydraulic traits of this subtropical tree species change across precipitation gradients and, how these traits vary with precipitation and phylogenetic differentiation among populations of *C. fargesii* remain unclear.

In this study, we investigated ten traits characterizing branch and leaf hydraulic architecture (Table 1) of mature trees from 12 *C. fargesii* populations in subtropical China, along an 1800-km-long gradient with a 570 mm difference in mean annual precipitation. We also conducted phylogenetic analyses to test the role of intraspecific phylogeny in hydraulic architecture adjustment. Our hypotheses were that (i) branch and leaf traits vary in a manner such that hydraulic efficiency (i.e. vessel diameter, theoretical hydraulic conductivity, vein density, stomatal density and stomatal pore index) decreases, while traits linked with hydraulic safety (i.e. wood density and turgor loss point) increases with decreasing precipitation; (ii) thus a tradeoff exists between hydraulic efficiency and safety, and hydraulic architectures of branch and leaf remain coordinated along the precipitation gradient; and (iii) intraspecific phylogeny plays a role in the variation and correlation of hydraulic architectures in *C. fargesii* along the precipitation gradient.

2. Materials and methods

2.1. Study sites and climate

The study was carried out in 12 natural *C. fargesii* populations across an 1800-km-long transect from the west to the east of subtropical China (Fig. 1, Table S1). Long-term (1970-2000) average values of precipitation were obtained from the WorldClim dataset (http://www.worldclim.org). Aridity index (AI) was calculated as the ratio of precipitation to potential evapotranspiration at a given site (Global-Aridity Geospatial Database; http://www.cgiar-csi.org).

2.2. Plant materials

Three to five mature *C. fargesii* individuals of similar size and height were selected from each population (Table S1). Branches and leaves were collected from the upper sun-exposed crown in July to August 2017, using a 16m-long sea fishing rod with a blade attached to the end. Samples were immediately put into zip-lock bags with a wet paper towel to avoid water loss. All samples were brought to the lab and stored in a fridge at 4 °C until hydraulic measurements were conducted.

2.3. Determinations of sapwood hydraulic architecture

Woody segments at about 40 cm below the branch apex and of 0.8–1 cm in diameters were used for the determinations (Martínez-Vilalta et al., 2009). Wood fresh volume with the bark removed was measured by water displacement and dry weight was measured after oven-dried at 105 °C for 72 h. Wood density (WD; g cm^{-3}) was then calculated as dry mass divided by fresh volume.

Transverse sections (25-35 μm in thickness) were prepared using a sliding microtome (Leica SM2010R; Leica Microsystems, Wetzlar, Germany), and stained with 1% safranin solution to enhance contrast between wood and the void space of vessels. For each section, six to over ten images per cross-section were taken at 4 × magnification using a light microscope (Leica DM2500; Leica Microsystems, Wetzlar, Germany) equipped with a high-resolution digital camera (Leica ICC50 W; Leica Microsystems, Wetzlar, Germany). These images were then combined to produce an integrated image covering the whole cross-section (or at least a radial transect according to the sectional quality), using the PTGui panorama stitching tool (http://www.ptgui.com). Since vessel diameter increases with cambial age (Carrer et al., 2015), to present the sapwood anatomical characteristics precisely, all the 1-, 2- and 3-year-old growth-rings of the whole cross-section were analyzed as a whole. Branch vessel density (BVD; n mm^{-2}), individual vessel diameter (*D*; μm) and vessel to sapwood area ratio (A_v/A_s; %) were determined using the particle analysis function of ImageJ (NIH, Bethesda, MD, USA). A total of 48 integrated images were obtained and a total of 141,169 vessels were measured.

According to the Hagen-Poiseuille law, a vessel's hydraulic conductivity increases with the fourth power of its diameter, making large vessels contribute disproportionately more to the overall hydraulic conductance (Tyree et al., 1994). To use a hydraulically meaningful index, we calculated the hydraulically weighted diameter (D_h; μm) (Tyree et al., 1994):

$$D_h = \left(\sum D^4/N\right)^{1/4}$$

where *N* is the total number of vessels in a integrated image, D_h is the mean diameter required to achieve the same overall conductance with the same number of vessels. Then the theoretical sapwood conductance (K_{th}; kg m^{-1} MPa^{-1} s^{-1}) was calculated according to the Hagen-

Table 1
The hydraulic variables with definitions, units and biological significance employed in this study.

Abbreviation	Definition	Unit	Significance
Branch hydraulic architecture			
WD	Wood density	g cm^{-3}	Index of mechanical properties, related to drought tolerance
A_v/A_s	Vessel to sapwood area ratio	%	Aare for water transport in xylem
BVD	Branch vessel density	n mm^{-2}	Water transport pathways in xylem
D_h	Hydraulically weighted vessel diameter, $D_h = (\Sigma D^4/N)^{1/4}$	μm	Trait determines water transport capacity in xylem, related to embolism resistance
K_{th}	Theoretical hydraulic conductivity, $K_{th} = (D_h{}^4\pi\rho/128\eta) \times$BVD	kg m^{-1} MPa^{-1} s^{-1}	Potential water transport capacity of xylem
VD	Vein density	mm mm^{-2}	Water transport pathways in leaves
SD	Stomatal density	n mm^{-2}	Water transpiration pathways on leaf surface
SL	Stomatal pore length	μm	Trait constrains water transpiration on leaf surface
SPI	Stomatal pore area index, SPI = SD × SL^2	–	Area for water transpiration on leaf surface
π_{tlp}	Leaf turgor loss point	MPa	Capability of leaves to maintain cell turgor pressure under water stress

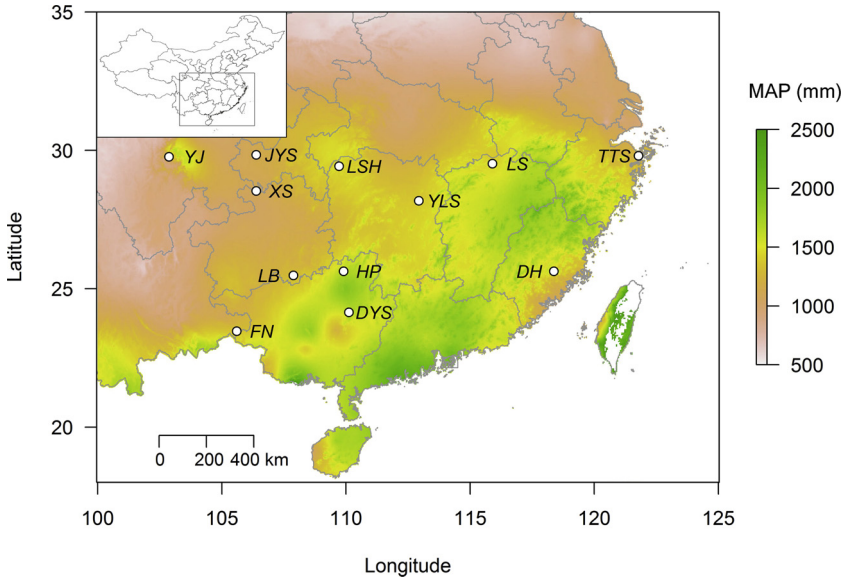

Fig. 1. Map of locations of 12 *Castanopsis fargesii* populations sampled in this study. For site codes and more information, see Table S1.

Poiseuille law:

$$K_{th} = \frac{D_h^4 \pi \rho}{128 \times \eta} \times \text{BVD}$$

where η is the viscosity of water at 20 °C (1.002×10^{-9} MPa s), ρ is the density of water at 20 °C (998.2 kg m^{-3}); the unit of D_h was transformed to m and BVD to m^{-2} before calculations.

2.4. Determinations of leaf hydraulic architecture

The water potential at the leaf turgor loss point (π_{tlp}; MPa) was determined by pressure-volume analysis, using the bench drying technique (Brodribb et al., 2003). Briefly, leafy branches were cut under water and rehydrated until leaf water potential (Ψ_L) was > −0.05 MPa, then one leaf per tree was detached for the determination of the pressure-volume curve (PV curve). In brief, leaves were first weighted to obtain the initial fresh mass, and then immediately placed in a pressure chamber (PMS, Corvallis, OR, USA) to determine the initial Ψ_L. Leaves were then allowed to desiccate slowly in the laboratory, and leaf mass and Ψ_L were measured periodically during the desiccation till wilting. After the PV curve measurements, dry mass of each measured leaf was weighted after oven-dried at 70 °C for 72 h, and leaf dry-matter content was calculated as the oven-dry mass of a leaf divided by its water-saturated fresh mass. The π_{tlp} was determined according to pressure volume relationship models based on a series of Ψ_L and corresponding leaf water content (Schulte and Hinckley, 1985). The π_{tlp} indicates the capability of leaves to maintain cell turgor and consequently biological functioning, such as stomatal and hydraulic conductance, photosynthesis and growth, under water stress (Brodribb et al., 2003; Brodribb and Holbrook, 2003).

Stomatal density (SD; n mm^{-2}) and stomatal pore length (SL; μm) were determined by microscopic measurement of imprints from abaxial nail varnish peels, one peel per leaf and three leaves per tree were used for the measurements. Total stomatal pore area index (SPI; a dimensionless index of stomatal pore area per leaf area) was calculated as SPI = SD × SL^2 (Sack et al., 2003). Vein density (VD; mm mm^{-2}) was obtained from the same leaves used for stomatal measurement. Briefly, patches about 1 cm^2 were cut from the middle part of leaves and soaked in 5% NaOH solution. After *c.* 10 days of soaking, the patches were cleaned and then stained with 1% safranin solution. Images of these patches were taken at 4× magnification (7.68 mm^2) and minor vein length was determined using ImageJ (NIH, Bethesda, MD, USA). VD was defined as total minor vein length per unit leaf area.

2.5. Intraspecific phylogenetic tree construction

We first extracted the haplotype data of the twelve populations from a previous study which was carried out in the same stands (Sun et al., 2014). Genetic distances between the twelve populations were then estimated using HAPLOTYPE ANALYSIS v.1.05 (Eliades and Eliades,

2009), the intra-specific phylogenetic tree was constructed using the R package *ape* (Paradis et al., 2004).

2.6. Statistical analyses

The hydraulic traits investigated are summarized in Table 1. All statistical analyses were performed with R version 3.4.3 (R Core Team, 2017). Regression relationships between plant traits and climatic factors were analyzed by linear mixed effect (LME) models using the R package *lme4* (Bates et al., 2015), with climatic factor as a fixed variable and different trees within a stand as a random effect, P-values were obtained by likelihood ratio tests of the full model with the effect in question against the model without the effect in question. In addition, backwards-stepwise regression was used to select the best-fitting equation from a starting set of input climatic factors. Linear relationships between plant traits were also analyzed with Pearson correlation coefficients, and multiple-trait relationships were analyzed by principal component analysis (PCA).

The Blomberg's *K*-statistic was calculated using the R package *Picante* (Kembel et al., 2010). The null assumption of the Blomberg's model is that a trait undergoes/evolves in a Brownian motion process with time, with Blomberg's $K = 1$ suggests that the trait distribution perfectly conforms to a Brownian motion model, while $K < 1$ implies a trait among population has a very weak phylogenetic signal and barely depends on the phylogenetic relationships, whereas $K > 1$ indicates a trait of closely related populations is more similar than expected under Brownian motion evolution (Blomberg et al., 2003). To test the phylogenetic effects on the correlations between traits, phylogenetically independent contrasts (PIC) were computed using the R package *ape* (Paradis et al., 2004). PIC uses phylogenetic information to transform inter-population data into phylogenetically independent data for further statistical analyses. Furthermore, the phylogenetic principal component analysis (PPCA, excluding the phylogenetic effects on multiple-trait relationships) was conducted using the R package *phytools* (Revell, 2012). For all the correlation and regression analyses, the results were accepted as significant when the probability of error (P) < 0.05.

3. Results

Across the precipitation gradients, MAP decreased from 1690 mm to 1120 mm and AI decreased from 1.55 to 1.14 (Table S1). Based on monthly data, the precipitation showed a distinct seasonality across sites, with relatively lower precipitation (9–30% of the MAP) in the dry season from November to March (Fig. S1). The AI also displayed a seasonality, particularly in the sites with lower MAP (Fig. S2).

According to the LME models, eight out of the ten traits were significantly related to precipitation ($P < 0.05$, Table 2). Specifically, three branch traits (i.e. wood density (WD), hydraulically weighted vessel diameter (D_h) and theoretical hydraulic conductivity (K_{th})) and all the five leaf traits were related to MAP, several traits were additionally related to AI and other precipitation variables (Table 2). The stepwise regression results further revealed that MAP was the major driver of variation in most traits, including two branch traits (i.e. D_h and K_{th}) and four leaf traits (i.e. vein density (VD), stomatal density (SD), stomatal pore area index (SPI) and turgor loss point (π_{tlp})) (r^2 = 0.32-0.69, $P < 0.037$, Table S2), while AI was the major driver of WD variance ($r^2 = 0.69$, $P < 0.001$, Table S2).

The most dramatic variation was found in K_{th}, which decreased by 74.3% from the wet end to the dry end ($P < 0.001$, Fig. 2a, Table S3). Decrease in K_{th} was caused by the decrease in D_h (by 31.9% from 60.3 to 41.0 μm; Fig. 2b, Table S3) rather than branch vessel density (BVD), which did not change with MAP (Table 2, Fig. 2c). WD increased significantly by 14.3% from 0.51 to 0.59 g cm^{-3} with decreasing MAP ($P < 0.01$, Fig. 2d). In addition, vessel diameter distributions were all right-skewed, with skewness between 1.4 and 2.5 (Fig. S3).

With decreasing MAP, leaf traits characterizing hydraulic efficiency declined significantly ($P < 0.05$, Fig. 3a, Table S3). Specifically, VD decreased by 14.6% from 8.6 to 7.3 mm mm^{-2} (Fig. 3a, Table S3). Stomatal density (SD) and stomatal pore length (SL) decreased by 10.5% and 12.0%, respectively (Table S3), leading to a 29.9% decrease in SPI (Fig. 3b). Leaf turgor loss point (π_{tlp}) declined by 51.3% from −1.51 to −2.29 MPa (Fig. 3c, Table S3).

According to the Pearson correlation analysis, K_{th}, D_h, SPI and VD were positively correlated (Fig. 4), indicating coordination between these traits. There was no significant correlation between D_h and BVD (Table S4). π_{tlp} was positively correlated with VD, SPI, K_{th} and D_h (Fig. 5, Table S4). The PCA result was consistent with the Pearson correlation result. Axis 1 accounted for 58.1% of total variation and was positively related to K_{th}, D_h, π_{tlp}, VD, SD, SL and SPI, and negatively related to WD (Fig. 6a), whereas Axis 2 accounted for 18.0% of total variation and was positively related to BVD and A_v/A_s (Fig. 6a).

Blomberg's *K* statistics in all traits were between 0.45 and 0.94 ($P > 0.127$), implying the observed patterns of traits among populations were consistent with those generated from a Brownian motion process, namely limited impacts of intraspecific phylogeny on the variation of these traits (Table 3). The PIC results were consistent with the Pearson correlation analysis using original data, except that the significance of a few coefficients differed slightly (Table S4). Moreover, the PPCA showed consistent result with the PCA (Fig. 6), indicating a minor if any impact of phylogeny on multiple-trait relationships.

Table 2
Results of linear mixed effect models shown the influence of precipitation variables (as fixed variables) on the hydraulic architecture in *Castanopsis fargesii*.

	MAP		AI		PET		Pmax		Pmin		Pwet		Pdry	
Variable	χ^2	*P*	χ^2	*P*	χ^2	*P*	χ^2	*P*	χ^2	*P*	χ^2	*P*	χ^2	*P*
WD	10.92	**0.001**	15.02	**0.000**	0.24	0.623	1.82	0.177	5.54	**0.019**	1.46	0.227	5.52	**0.019**
A_v/A_s	1.09	0.296	0.00	0.963	2.95	0.086	2.24	0.134	0.03	0.868	2.18	0.140	0.07	0.797
BVD	0.54	0.463	0.22	0.638	0.49	0.483	0.00	0.988	0.89	0.344	0.10	0.751	0.85	0.356
D_h	10.88	**0.001**	4.73	**0.030**	3.96	**0.047**	7.28	**0.007**	1.97	0.161	7.22	**0.007**	1.92	0.166
K_{th}	14.43	**0.000**	6.64	**0.010**	3.79	0.052	6.14	**0.013**	3.34	0.068	5.26	**0.022**	3.05	0.081
VD	13.84	**0.000**	10.45	**0.001**	1.55	0.213	4.50	**0.034**	3.79	0.051	3.39	0.066	3.79	0.052
SD	7.96	**0.005**	7.13	**0.008**	0.56	0.456	1.92	0.166	5.29	**0.021**	1.77	0.183	4.11	**0.043**
SL	5.21	**0.023**	1.33	0.249	6.14	**0.013**	5.02	**0.025**	0.11	0.736	4.43	**0.035**	0.09	0.769
SPI	10.64	**0.001**	4.67	**0.031**	3.77	0.052	4.95	**0.026**	1.88	0.171	4.37	**0.037**	1.45	0.229
π_{tlp}	14.05	**0.000**	7.02	**0.008**	4.52	**0.034**	9.27	**0.002**	1.44	0.230	9.04	**0.003**	1.48	0.224

χ^2: likehood ratio; *P*: probability of error. Significant correlations ($P < 0.05$) are shown in bold underlined text. WD: wood density; A_v/A_s: vessel to sapwood area ratio; BVD: branch vessel density; D_h: hydraulically weighted vessel diameter; K_{th}: theoretical hydraulic conductivity; VD: vein density; SD: stomatal density; SL: stomatal pore length; SPI: stomatal pore area index; π_{tlp}: leaf turgor loss point. MAP: mean annual sum precipitation; AI: aridity index; PET: mean annual potential evapotranspiration; Pmax: precipitation of the wettest month; Pmin: precipitation of the driest month; Pwet: precipitation of the wettest quarter; Pdry: precipitation of the driest quarter.

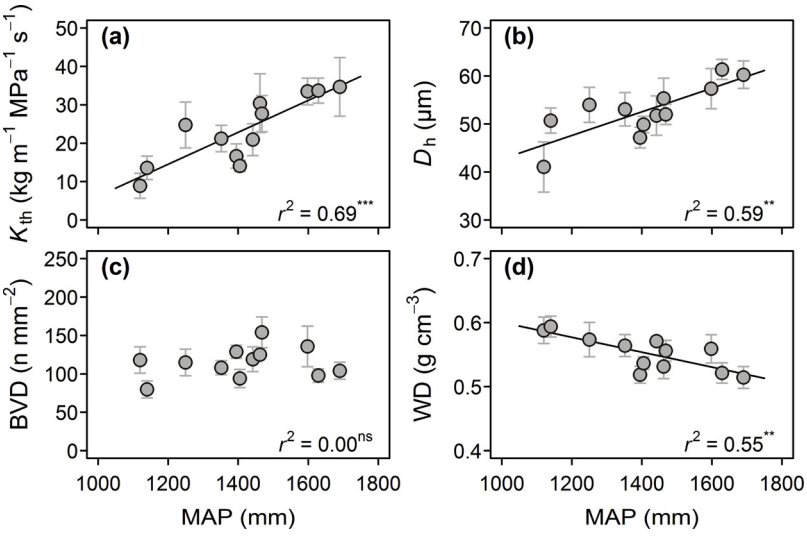

Fig. 2. Relationships between branch hydraulic architecture and mean annual precipitation (MAP) in *Castanopsis fargesii*. MAP in relation to theoretical sapwood conductance (K_{th}; a), hydraulically weighted vessel diameter (D_h; b), branch vessel density (BVD; c), and wood density (WD; d). Linear regression lines are shown, with the adjusted r^2. Statistical significance is indicated by asterisks: ns, $P > 0.05$; **, $P < 0.01$; ***, $P < 0.001$. Error bars represent ± SE.

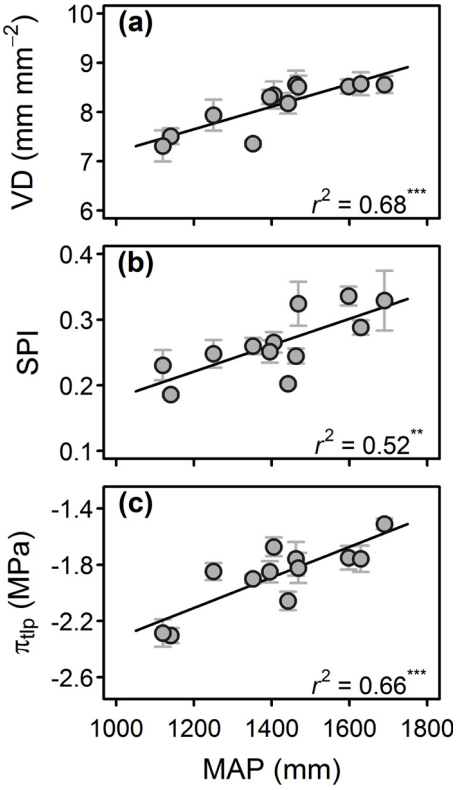

Fig. 3. Relationships between leaf hydraulic architecture and mean annual precipitation (MAP) in *Castanopsis fargesii*. MAP in relation to leaf vein density (VD; a), stomatal pore area index (SPI; b) and turgor loss point (π_{tlp}; c). Linear regression lines are shown, with the adjusted r^2. Statistical significance is indicated by asterisks: **, $P < 0.01$; ***, $P < 0.001$. Error bars represent ± SE.

4. Discussion

4.1. Branch hydraulic architecture in relation to precipitation

Across *C. fargesii* populations, as predicted, theoretical hydraulic conductivity (K_{th}) decreased markedly with decreasing precipitation. This indicates that sapwood hydraulic efficiency is lower at drier sites, which is in line with previous studies (Hajek et al., 2016; Pfautsch et al., 2016). We found that K_{th} declined in parallel with hydraulically weighted vessel diameter (D_h), while branch vessel density (BVD) did not change with precipitation, indicating that water transport in xylem of *C. fargesii* adapts to precipitation mainly by regulating vessel diameter, rather than vessel density. Similarly, it was reported that vessel density of *Fagus sylvatica* (Schuldt et al., 2016) and tracheid density of *Pinus sylvestris* (Martínez-Vilalta et al., 2009) did not vary with precipitation. Also consistent with our results, D_h decreased with decreasing precipitation in some boreal and temperate species (Villar-Salvador et al., 1997; Schreiber et al., 2015). However, D_h did not vary with precipitation in some deciduous Fagaceae species, such as *Quercus faginea* (Villar-Salvador et al., 1997) and *Fagus sylvatica* (Schuldt et al., 2016). Thus it seems that sapwood adapts to precipitation differently between evergreen (including *C. fargesii* in our study) and deciduous Fagaceae species.

The D_h of the subtropical *C. fargesii* was 40–60 μm, which is greater than those of trees from desert, temperate and boreal sites (with a upper boundary of about 30 μm), while is much lower than those of species from tropical rain forest (up to 125 μm) (Hacke et al., 2017). However, it is notable that *C. fargesii* is a ring-porous tree species that possess a high proportion of narrow vessels (Woodcock, 1989), resulting in a right skewed (longer right tail) distribution of vessel diameters (Fig. S3). An abundance of narrow vessels might be important under the scenario of a distinct rainfall seasonality in subtropical China (Wang et al., 2005). While contributing little to water transport during the wet season, these narrow vessels in *C. fargesii* can provide alternate pathways when large vessels become embolized, thus constituting a safeguard against water deficit during the dry season (Carlquist, 1980). We also noted that between two driest sites (Jinyunshan and Xishui), D_h decreased 10 μm (Table S3) while MAP only decreased 20 mm (Table S1). Such an intriguing effect may be contributed by the differences of environmental factors beside precipitation, such as temperature. In a warming experiment, elevated temperature (+3.4 °C) significantly increased vessel diameters of *Abies balsamea*, *Acer saccharum* and *Quercus macrocarpa* in the temperate-boreal ecotone (McCulloh et al., 2016), and it was also reported that vessel diameters of *Q. macrocarpa* are positively related with the growing season temperature (Voelker et al., 2012). Indeed, the mean annual temperature was lower at Xishui (14.6 °C) than at Jinyunshan (16.0 °C), due to a higher latitude at Xishui (1228 m) than at Jinyunshan (412 m) (Table S1).

Wood density (WD), which has been widely assumed to relate to xylem hydraulic vulnerability (Hacke et al., 2001; Dalla-Salda et al., 2011; Menezes-Silva et al., 2015), was reported to increase with decreasing water availability at the interspecific level (Ibanez et al., 2017). At the intraspecific level, here we found that WD of *C. fargesii* increased linearly with decreasing MAP and AI. This may indicate that xylem cavitation resistance of *C. fargesii* increased in response to

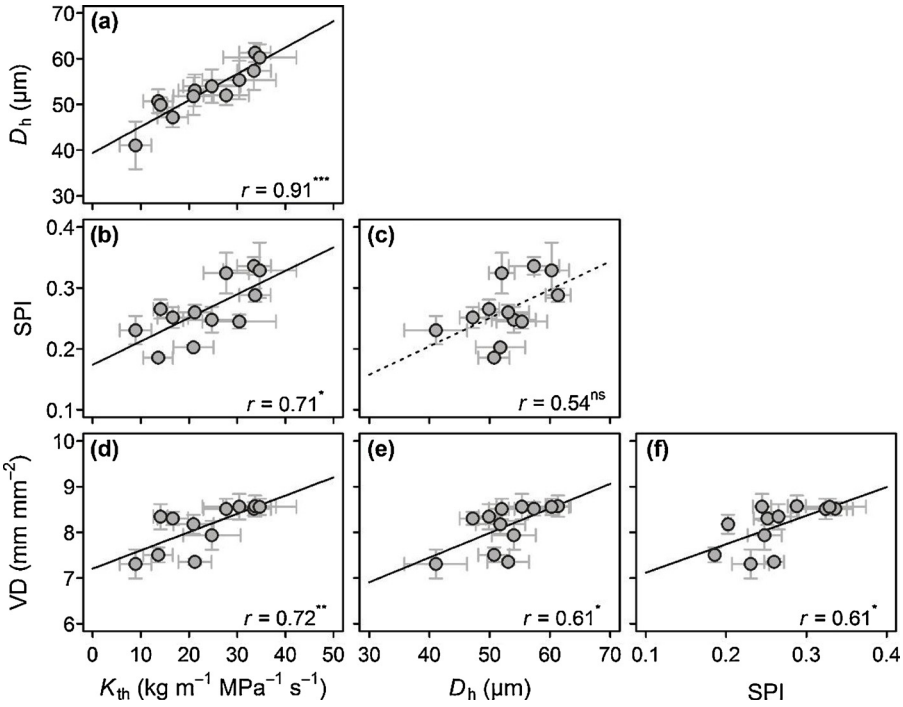

Fig. 4. Correlations between branch and leaf hydraulic architectures in *Castanopsis fargesii*. Theoretical sapwood conductance (K_{th}) in relation to hydraulically weighted vessel diameter (D_h; a), stomatal pore area index (SPI; b) and vein density (VD; d); D_h in relation to SPI (c) and VD (e); SPI in relation to VD (f). Linear regression lines are shown, with the Pearson correlation coefficients *r*. Statistical significance is indicated by asterisks: ns, $P > 0.05$; *, $P < 0.05$; **, $P < 0.01$; ***, $P < 0.001$. Error bars represent ± SE.

decreasing precipitation. While not all species decrease WD with decreasing precipitation (e.g. Schuldt et al., 2016), results from common garden experiments showed that the response of WD to precipitation gradient may be species specific (Nabais et al., 2018). This is because WD is determined not only by water availability, but also by other factors such as temperature (Zhang et al., 2013) and soil fertility (Heineman et al., 2016).

4.2. Leaf hydraulic architecture in relation to precipitation

We found that vein density (VD) of *C. fargesii* decreased linearly with decreasing MAP, in parallel with decreases in stomatal density (SD), stomatal pore length (SL) and stomatal pore area index (SPI). These results indicate that leaf water transport capacity decreased with decreasing precipitation, which is in line with our expectations. It has been shown that higher VD could transport larger volumes of water (Brodribb et al., 2007; Brodribb and Feild, 2010), suggesting that higher VD under higher precipitation can facilitate water supply at the leaf level. However, some opposite results have also been reported, namely VD increased with decreasing MAP across species regionally (Schneider et al., 2018) and globally (Sack and Scoffoni, 2013), though with relatively low coefficients. Higher VD in drier areas has been thought, on one hand, to facilitate water transport during the period with high water availability (Sack and Scoffoni, 2013). On the other hand, it has been assumed that higher VD is related to higher leaf drought resistance, because higher VD provides more alternative water pathways, water transport can be maintained even embolism occurs in part of leaf veins (Scoffoni et al., 2011). In our study, however, VD and turgor loss point (π_{tlp}) were positively related, indicating that leaves had higher VD were less drought resistant, and hence this assumption is not valid in *C. fargesii*.

Both stomatal density (SD) and stomatal pore length (SL) decreased with decreasing precipitation in *C. fargesii*, whereas they were not significantly correlated, in contrast with previous reports that SD and SL are negatively correlated at both inter- and intraspecific level (Franks and Beerling, 2009; Li et al., 2015a; Dittberner et al., 2018). For example, a recent study reported that SD decreased while stomatal size increased with decreasing MAP across species from cold temperate to tropical forests in China (Liu et al., 2018). However, there is not necessarily an inherent correlation between stomatal density and size because, in theory, many combinations of stomatal density and size yield the same stomatal conductance (Franks et al., 2009). In *C. fargesii* across the precipitation gradient, SPI was positively related with SL but not with SD (Table S4), the higher SPI was driven more by SL than by SD.

Another key finding of this study is that turgor loss point (π_{tlp})

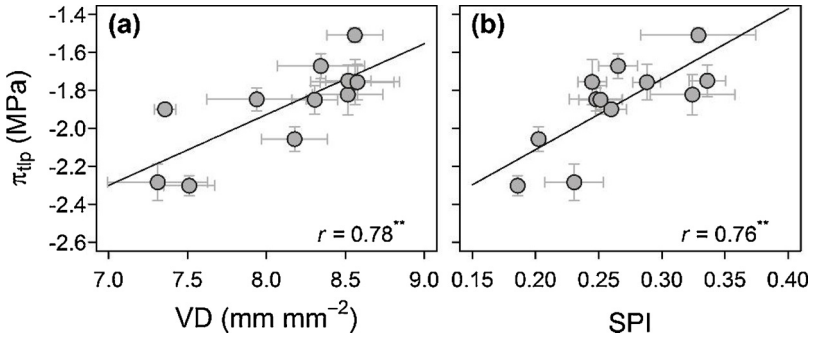

Fig. 5. Leaf turgor loss point (π_{tlp}) in relation to vein density (VD; a) and stomatal pore area index (SPI; b) in *Castanopsis fargesii*. Linear regression lines are shown, with the Pearson correlation coefficients *r*. Statistical significance is indicated by asterisks: **, $P < 0.01$. Error bars represent ± SE.

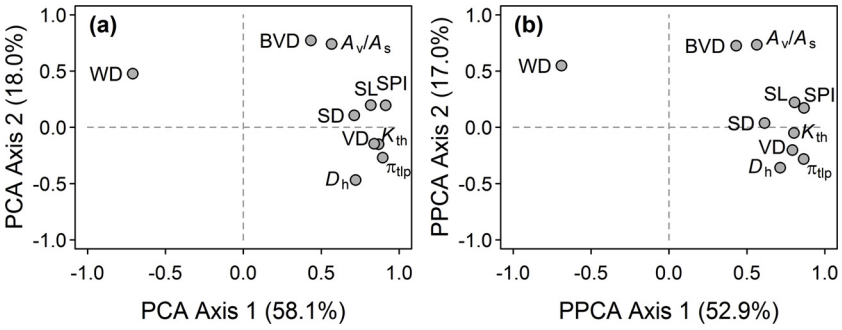

Fig. 6. Results of principal component analysis (PCA; a) and phylogenetic principal component analysis (PPCA; b) on multiple-trait relationships in *Castanopsis fargesii*. WD: wood density; A_v/A_s: vessel to sapwood area ratio; BVD: branch vessel density; D_h: hydraulically weighted vessel diameter; K_{th}: theoretical hydraulic conductivity; VD: vein density; SD: stomatal density; SL: stomatal pore length; SPI: stomatal pore area index; π_{tlp}: leaf turgor loss point.

decreased linearly with decreasing precipitation, suggesting that the capability of leaves to maintain cell turgor pressure (and consequently biological functioning such as water and gas exchange) increases with decreasing precipitation in *C. fargesii*. To our knowledge, this is the first report that a linear decrease in π_{tlp} was observed with decreasing precipitation within a single tree species. Previous studies have demonstrated that species growing in drier regions had more negative values of π_{tlp} (Lenz et al., 2006; Bartlett et al., 2012; Zhu et al., 2018). Our results are in agreement with these interspecific observations, and indicate that leaves of *C. fargesii* from drier sites can maintain water conductivity and CO_2 exchange under lower water availability.

4.3. Coordination and trade-off between hydraulic traits

We found a strong coordination among traits characterizing hydraulic efficiency of branches (i.e. K_{th} and D_h) and leaves (i.e. VD and SPI, Fig. 4). These results suggest a coordinated adjustment of branch and leaf hydraulic systems in *C. fargesii* across the precipitation gradient. However, we did not find a coordination between VD and SD, which has been reported both within and across species (Brodribb and Jordan, 2011; Franks et al., 2012; Carins Murphy et al., 2014; Li et al., 2015a). Nonetheless, VD was positively related with SPI, indicating a coordination between water supply and evaporation demand in *C. fargesii* leaves. This argument is further strengthened by the PCA result that trees had traits conferring higher water transport efficiency (D_h, K_{th} and VD) also had traits conferring higher water loss rate (SD, SL and SPI) (Fig. 6). Our results highlight the strong coordination between hydraulic systems regulating water delivery (i.e., branch and leaf xylem) and water loss (i.e., stomata), which can help to maintain the leaf water content at a relatively constant level, and thus protect against damage to photosynthetic and xylem tissues (Brodribb et al., 2017).

A trade-off between plant hydraulic efficiency and safety has been confirmed such as in xylem (Gleason et al., 2015) and leaves across species (Scoffoni and Sack, 2017). Although hydraulic safety is commonly expressed as the water potential causing 50% loss of hydraulic conductivity (P50), with the more negative P50, the higher hydraulic safety (Choat et al., 2012), π_{tlp} was also proved to be a good proxy of leaf P50 (Blackman et al., 2010; Zhu et al., 2018). We found that π_{tlp} was positively related to VD and SPI (Fig. 5), suggesting that a trade-off between hydraulic efficiency and safety does exist at the leaf level in *C. fargesii* grown along the precipitation gradient. Since leaves with higher vein density were less drought tolerant (i.e., less negative π_{tlp}, Fig. 5), increase of leaf vein density in *C. fargesii* might be related to increase of leaf hydraulic efficiency, rather than increase of hydraulic safety (Blackman et al., 2018).

4.4. Limited phylogenetic influences on hydraulic architecture

Contrary to our expectation, the effect of intraspecific phylogeny on the variation of hydraulic architecture in *C. fargesii* was limited. None of the tested hydraulic traits exhibited a significant phylogenetic signal with the Blomberg's $K < 1$, whereas they varied significantly with precipitation, indicating that the variation of hydraulic architecture in this species is primarily due to phenotypic plasticity. Phylogenetic analyses have not been used in studies of intraspecific variation in plant traits until more recently, a study conducted by Rungwattana et al. (2018) reported similar results, i.e., the Blomberg's $K < 1$ for all studied traits in a tropical tree species, *Hevea brasiliensis*. A high degree of phenotypic plasticity of hydraulic traits was also observed in other species, for example, vessel diameter in *Populus tremuloides* (Schreiber et al., 2015) and xylem cavitation resistance in *Fagus sylvatica* (Wortemann et al., 2011) and *Pinus pinaster* (Corcuera et al., 2011). We argue that phenotypic plasticity plays a key role in the variation of hydraulic architecture in *C. fargesii* across the precipitation gradient,

Table 3
Phylogenetic signals of the ten hydraulic traits in *Castanopsis fargesii* indicated by the Blomberg's *K* statistic.

Variable	Blomberg's *K*	PIC.variance.obs	PIC.variance.rnd.mean	PIC.variance.P
Branch hydraulic architecture				
WD	0.836	0.00	0.00	0.137
A_v/A_s	0.736	2.18	2.82	0.301
BVD	0.940	1598.86	2239.48	0.203
D_h	0.446	222.02	170.70	0.854
K_{th}	0.527	450.59	430.76	0.645
Leaf hydraulic architecture				
VD	0.504	1.46	1.34	0.672
SD	0.815	1071.78	1586.94	0.127
SL	0.614	10.66	11.77	0.466
SPI	0.736	0.01	0.01	0.250
π_{tlp}	0.538	0.31	0.31	0.593

PIC.variance.obs: the observed phylogenetically independent contrast variance of a trait. PIC.variance.rnd.mean: the mean variation of independent contrasts of a null model. PIC.variance.P: the quantile of PIC.variance.obs versus PIC.variance.rnd.mean, represents the statistical significance of phylogenetic signal, traits with PIC.variance.P < 0.05 have non-random phylogenetic signal. WD: wood density; A_v/A_s: vessel to sapwood area ratio; BVD: branch vessel density; D_h: hydraulically weighted vessel diameter; K_{th}: theoretical hydraulic conductivity; VD: vein density; SD: stomatal density; SL: stomatal pore length; SPI: stomatal pore area index; π_{tlp}: leaf turgor loss point.

conferring this tree species with a great ability to respond to changes in water availability.

Drivers of variation in hydraulic traits across environments within and between species could be different. In contrast to our intraspecific phylogenetic analyses, phylogenetic signals of hydraulic architectures were strong in 27 Magnoliaceae species (Liu et al., 2015). Similarly, studies carried out on 23 *Callitris* species (Larter et al., 2017) and 28 *Eucalyptus* species (Pfautsch et al., 2016) showed that species from drier habitats had smaller D_h, and differences in hydraulic traits were largely due to genotypic differences rather than phenotypic plasticity (Pfautsch et al., 2016). However, genetic differences are much smaller within a single species than across species, thus the effects of phenotypic plasticity on plant hydraulics seem to be more prominent in *C. fargesii* in the present study.

5. Conclusions

As a dominant tree species in subtropical forests, *C. fargesii* modified branch and leaf hydraulic architectures in a coordinated manner along the precipitation gradient. Individuals in wetter habitats had traits that conferred higher water transport efficiency, while individuals in drier habitats had traits associated with higher drought tolerance and higher water use efficiency. Rather than being caused by intraspecific phylogeny, the variation in hydraulics of *C. fargesii* is primarily due to phenotypic plasticity, suggesting that precipitation has dominant influences on the variation of plant hydraulics in this species. We conclude that the precipitation driven variation in hydraulic architecture would confer *C. fargesii* with a high degree of plasticity to respond to the shifts in precipitation under future climate change. Hence, in practice, *C. fargesii* can be used as a potential tree species for reforestation to cope with climate change in subtropical China.

Authors' contributions

Q.Y., P.C.H. and S.D.Z. designed the research; X.Y.L., P.C.H., S.D.Z., G.L.W., H.Z. and Z.T.Y. collected the samples; X.Y.L., P.C.H., H.H. and Y.Y.X. determined the traits; X.Y.L. and H.L. analyzed the data; X.Y.L., P.C.H., H.L., I.K.U. and Q.Y. wrote the manuscript.

Acknowledgements

This work was supported by the National Natural Science Foundation of China [31800336; 31570405], the National Basic Research Program of China [2013CB956704], and the CAS/SAFEA International Partnership Program for Creative Research Teams. We thank Ye Sun and Chun Li for their help in samplings, and Zhengfeng Wang for his help in constructing the phylogenetic tree. We also thank the two anonymous reviewers for their helpful suggestions and comments on the manuscript. The authors declare no conflict of interest.

Appendix A. Supplementary data

Supplementary material related to this article can be found, in the online version, at doi:https://doi.org/10.1016/j.agrformet.2019.02.043.

References

Anderegg, W.R., Klein, T., Bartlett, M., Sack, L., Pellegrini, A.F., Choat, B., et al., 2016. Meta-analysis reveals that hydraulic traits explain cross-species patterns of drought-induced tree mortality across the globe. Proc. Natl. Acad. Sci. U. S. A. 113, 5024–5029.

Bartlett, M.K., Scoffoni, C., Sack, L., 2012. The determinants of leaf turgor loss point and prediction of drought tolerance of species and biomes: a global meta-analysis. Ecol. Lett. 15, 393–405.

Bates, D., Maechler, M., Bolker, B., Walker, S., 2015. Fitting linear mixed-effects models using lme4. J. Stat. Software 67, 1–48.

Blackman, C.J., Brodribb, T.J., Jordan, G.J., 2010. Leaf hydraulic vulnerability is related to conduit dimensions and drought resistance across a diverse range of woody angiosperms. New Phytol. 188, 1113–1123.

Blackman, C.J., Gleason, S.M., Cook, A.M., Chang, Y., Laws, C.A., Westoby, M., 2018. The links between leaf hydraulic vulnerability to drought and key aspects of leaf venation and xylem anatomy among 26 Australian woody angiosperms from contrasting climates. Ann. Bot. 122, 59–67.

Blomberg, S.P., Garland, T., Ives, A.R., Crespi, B., 2003. Testing for phylogenetic signal in comparative data: behavioral traits are more labile. Evolution 57, 717–745.

Blonder, B., Salinas, N., Bentley, L.P., Shenkin, A., Porroa, P.O.C., Tejeira, Y.V., et al., 2017. Predicting trait-environment relationships for venation networks along an Andes-Amazon elevation gradient. Ecology 98, 1239–1255.

Brodribb, T.J., Feild, T.S., 2010. Leaf hydraulic evolution led a surge in leaf photosynthetic capacity during early angiosperm diversification. Ecol. Lett. 13, 175–183.

Brodribb, T.J., Holbrook, N.M., 2003. Stomatal closure during leaf dehydration, correlation with other leaf physiological traits. Plant Physiol. 132, 2166–2173.

Brodribb, T.J., Jordan, G.J., 2011. Water supply and demand remain balanced during leaf acclimation of *Nothofagus cunninghamii* trees. New Phytol. 192, 437–448.

Brodribb, T., Holbrook, N., Edwards, E., Gutierrez, M., 2003. Relations between stomatal closure, leaf turgor and xylem vulnerability in eight tropical dry forest trees. Plant Cell Environ. 26, 443–450.

Brodribb, T.J., Feild, T.S., Jordan, G.J., 2007. Leaf maximum photosynthetic rate and venation are linked by hydraulics. Plant Physiol. 144, 1890–1898.

Brodribb, T.J., McAdam, S.A., Murphy, M.R.C., 2017. Xylem and stomata, coordinated through time and space. Plant Cell Environ. 40, 872–880.

Cai, J., Tyree, M.T., 2010. The impact of vessel size on vulnerability curves: data and models for within-species variability in saplings of aspen, *Populus tremuloides* Michx. Plant Cell Environ. 33, 1059–1069.

Carins Murphy, M.R., Jordan, G.J., Brodribb, T.J., 2014. Acclimation to humidity modifies the link between leaf size and the density of veins and stomata. Plant Cell Environ. 37, 124–131.

Carlquist, S., 1980. Further concepts in ecological wood anatomy, with comments on recent work in wood anatomy and evolution. Aliso J. Syst. Evol. Bot. 9, 499–553.

Carrer, M., von Arx, G., Castagneri, D., Petit, G., 2015. Distilling allometric and environmental information from time series of conduit size: the standardization issue and its relationship to tree hydraulic architecture. Tree Physiol. 35, 27–33.

Choat, B., Cobb, A.R., Jansen, S., 2008. Structure and function of bordered pits: new discoveries and impacts on whole-plant hydraulic function. New Phytol. 177, 608–626.

Choat, B., Jansen, S., Brodribb, T.J., Cochard, H., Delzon, S., Bhaskar, R., et al., 2012. Global convergence in the vulnerability of forests to drought. Nature 491, 752–755.

Choat, B., Brodribb, T.J., Brodersen, C.R., Duursma, R.A., López, R., Medlyn, B.E., 2018. Triggers of tree mortality under drought. Nature 558, 531–539.

Christman, M.A., Sperry, J.S., Adler, F.R., 2009. Testing the 'rare pit' hypothesis for xylem cavitation resistance in three species of Acer. New Phytol. 182, 664–674.

Corcuera, L., Cochard, H., Gil-Pelegrin, E., Notivol, E., 2011. Phenotypic plasticity in mesic populations of *Pinus pinaster* improves resistance to xylem embolism (P_{50}) under severe drought. Trees 25, 1033–1042.

Dalla-Salda, G., Martinez-Meier, A., Cochard, H., Rozenberg, P., 2011. Genetic variation of xylem hydraulic properties shows that wood density is involved in adaptation to drought in Douglas-fir (*Pseudotsuga menziesii* (Mirb.)). Ann. For. Sci. 68, 747–757.

Dittberner, H., Korte, A., Mettler-Altmann, T., Weber, A., Monroe, G., de Meaux, J., 2018. Natural Variation in Stomata Size Contributes to the Local Adaptation of Water-Use Efficiency in *Arabidopsis thaliana*. bioRxiv.

Eliades, N.G., Eliades, D.G., 2009. HAPLOTYPE ANALYSIS: Software for Analysis of Haplotype Data. Georg-August University Goettingen, Germany.

Franks, P.J., Beerling, D.J., 2009. Maximum leaf conductance driven by CO_2 effects on stomatal size and density over geologic time. Proc. Natl. Acad. Sci. 106, 10343–10347.

Franks, P.J., Drake, P.L., Beerling, D.J., 2009. Plasticity in maximum stomatal conductance constrained by negative correlation between stomatal size and density: an analysis using *Eucalyptus globulus*. Plant Cell Environ. 32, 1737–1748.

Franks, P.J., Leitch, I.J., Ruszala, E.M., Hetherington, A.M., Beerling, D.J., 2012. Physiological framework for adaptation of stomata to CO_2 from glacial to future concentrations. Philos. Trans. R. Soc. B Biol. Sci. 367, 537–546.

Gleason, S.M., Westoby, M., Jansen, S., Choat, B., Hacke, U.G., Pratt, R.B., et al., 2015. Weak tradeoff between xylem safety and xylem-specific hydraulic efficiency across the world's woody plant species. New Phytol. 209, 123–136.

Hacke, U.G., Sperry, J.S., 2001. Functional and ecological xylem anatomy. Perspect. Plant Ecol. Evol. Syst. 4, 97–115.

Hacke, U.G., Sperry, J.S., Pockman, W.T., Davis, S.D., McCulloh, K.A., 2001. Trends in wood density and structure are linked to prevention of xylem implosion by negative pressure. Oecologia 126, 457–461.

Hacke, U.G., Sperry, J.S., Wheeler, J.K., Castro, L., 2006. Scaling of angiosperm xylem structure with safety and efficiency. Tree Physiol. 26, 689–701.

Hacke, U.G., Spicer, R., Schreiber, S.G., Plavcová, L., 2017. An ecophysiological and developmental perspective on variation in vessel diameter. Plant Cell Environ. 40, 831–845.

Hajek, P., Kurjak, D., von Wühlisch, G., Delzon, S., Schuldt, B., 2016. Intraspecific variation in wood anatomical, hydraulic, and foliar traits in ten European beech provenances differing in growth yield. Front. Plant Sci. 7, 791.

Heineman, K.D., Turner, B.L., Dalling, J.W., 2016. Variation in wood nutrients along a tropical soil fertility gradient. New Phytol. 211, 440–454.

Ibanez, T., Chave, J., Barrabé, L., Elodie, B., Boutreux, T., Trueba, S., et al., 2017. Community variation in wood density along a bioclimatic gradient on a hyper-diverse tropical island. J. Veg. Sci. 28, 19–33.

Jacobsen, A.L., Pratt, R.B., Ewers, F.W., Davis, S.D., 2007. Cavitation resistance among 26

chaparral species of southern California. Ecol. Monogr. 77, 99–115.
Jansen, S., Choat, B., Pletsers, A., 2009. Morphological variation of intervessel pit membranes and implications to xylem function in angiosperms. Am. J. Bot. 96, 409–419.
Kembel, S.W., Cowan, P.D., Helmus, M.R., Cornwell, W.K., Morlon, H., Ackerly, D.D., et al., 2010. Picante: R tools for integrating phylogenies and ecology. Bioinformatics 26, 1463–1464.
Larter, M., Pfautsch, S., Domec, J.-C., Trueba, S., Nagalingum, N., Delzon, S., 2017. Aridity drove the evolution of extreme embolism resistance and the radiation of conifer genus Callitris. New Phytol. 215, 97–112.
Lenz, T.I., Wright, I.J., Westoby, M., 2006. Interrelations among pressure–volume curve traits across species and water availability gradients. Physiol. Plant. 127, 423–433.
Li, C., Sun, Y., Huang, H.W., Cannon, C.H., 2014. Footprints of divergent selection in natural populations of *Castanopsis fargesii* (Fagaceae). Heredity 113, 533–541.
Li, L., McCormack, M.L., Ma, C., Kong, D., Zhang, Q., Chen, X., et al., 2015a. Leaf economics and hydraulic traits are decoupled in five species-rich tropical-subtropical forests. Ecol. Lett. 18, 899–906.
Li, R.H., Zhu, S.F., Chen, H.Y., John, R., Zhou, G.Y., Zhang, D.Q., et al., 2015b. Are functional traits a good predictor of global change impacts on tree species abundance dynamics in a subtropical forest? Ecol. Lett. 18, 1181–1189.
Liu, H., Xu, Q.Y., He, P.C., Santiago, L.S., Yang, K.M., Ye, Q., 2015. Strong phylogenetic signals and phylogenetic niche conservatism in ecophysiological traits across divergent lineages of Magnoliaceae. Sci. Rep. 5, 12246.
Liu, C., He, N., Zhang, J., Li, Y., Wang, Q., Sack, L., et al., 2018. Variation of stomatal traits from cold temperate to tropical forests and association with water use efficiency. Funct. Ecol. 32, 20–28.
Maherali, H., Pockman, W.T., Jackson, R.B., 2004. Adaptive variation in the vulnerability of woody plants to xylem cavitation. Ecology 85, 2184–2199.
Martínez-Vilalta, J., Cochard, H., Mencuccini, M., Sterck, F., Herrero, A., Korhonen, J.F.J., et al., 2009. Hydraulic adjustment of Scots pine across Europe. New Phytol. 184, 353–364.
McCulloh, K.A., Petitmermet, J., Stefanski, A., Rice, K.E., Rich, R.L., Montgomery, R.A., et al., 2016. Is it getting hot in here? Adjustment of hydraulic parameters in six boreal and temperate tree species after 5 years of warming. Glob. Change Biol. 22, 4124–4133.
McDowell, N., Pockman, W.T., Allen, C.D., Breshears, D.D., Cobb, N., Kolb, T., et al., 2008. Mechanisms of plant survival and mortality during drought: why do some plants survive while others succumb to drought? New Phytol. 178, 719–739.
Menezes-Silva, P.E., Cavatte, P.C., Martins, S.C.V., Reis, J.V., Pereira, L.F., Ávila, R.T., et al., 2015. Wood density, but not leaf hydraulic architecture, is associated with drought tolerance in clones of *Coffea canephora*. Trees 29, 1687–1697.
Nabais, C., Hansen, J.K., David-Schwartz, R., Klisz, M., López, R., Rozenberg, P., 2018. The effect of climate on wood density: what provenance trials tell us? For. Ecol. Manage. 408, 148–156.
Niewiarowski, P.H., Angilletta, M.J., Leaché, A.D., 2004. Phylogenetic comparative analysis of life-history variation among populations of the lizard sceloporus undulatus: an example and prognosis. Evolution 58, 619–633.
Olave, M., Avila, L.J., Sites, J.W., Morando, M., 2017. Hidden diversity within the lizard genus Liolaemus: genetic vs morphological divergence in the L. rothi complex (Squamata:Liolaeminae). Mol. Phylogenet. Evol. 107, 56–63.
Paradis, E., Claude, J., Strimmer, K., 2004. APE: analyses of phylogenetics and evolution in R language. Bioinformatics 20, 289–290.
Pfautsch, S., Harbusch, M., Wesolowski, A., Smith, R., Macfarlane, C., Tjoelker, M.G., et al., 2016. Climate determines vascular traits in the ecologically diverse genus *Eucalyptus*. Ecol. Lett. 19, 240–248.
Ramírez-Valiente, J.A., Deacon, N.J., Etterson, J., Center, A., Sparks, J.P., Sparks, K.L., et al., 2018. Natural selection and neutral evolutionary processes contribute to genetic divergence in leaf traits across a precipitation gradient in the tropical oak *Quercus oleoides*. Mol. Ecol. 27, 2176–2192.
Revell, L.J., 2012. Phytools: an R package for phylogenetic comparative biology (and other things). Methods Ecol. Evol. 3, 217–223.
Rungwattana, K., Kasemsap, P., Phumichai, T., Kanpanon, N., Rattanawong, R., Hietz, P., 2018. Trait evolution in topical rubber (*Hevea brasiliensis*) trees is related to dry season intensity. Funct. Ecol. 32, 2638–2651.
Sack, L., Scoffoni, C., 2013. Leaf venation: structure, function, development, evolution, ecology and applications in the past, present and future. New Phytol. 198, 983–1000.
Sack, L., Cowan, P.D., Jaikumar, N., Holbrook, N.M., 2003. The 'hydrology' of leaves: co-ordination of structure and function in temperate woody species. Plant Cell Environ. 26, 1343–1356.
Schneider, J.V., Negraschis, V., Habersetzer, J., Rabenstein, R., Wesenberg, J., Wesche, K., et al., 2018. Taxonomic diversity masks leaf vein–climate relationships: lessons from herbarium collections across a latitudinal rainfall gradient in West Africa. Bot. Lett. 165, 384–395.
Schreiber, S.G., Hacke, U.G., Hamann, A., 2015. Variation of xylem vessel diameters across a climate gradient: insight from a reciprocal transplant experiment with a widespread boreal tree. Funct. Ecol. 29, 1392–1401.
Schuldt, B., Knutzen, F., Delzon, S., Jansen, S., Müller-Haubold, H., Burlett, R., et al., 2016. How adaptable is the hydraulic system of European beech in the face of climate change-related precipitation reduction? New Phytol. 210, 443–458.
Schulte, P.J., Hinckley, T.M., 1985. A comparison of pressure-volume curve data analysis techniques. J. Exp. Bot. 36, 1590–1602.
Scoffoni, C., Sack, L., 2017. The causes and consequences of leaf hydraulic decline with dehydration. J. Exp. Bot. 68, 4479–4496.
Scoffoni, C., Rawls, M., McKown, A., Cochard, H., Sack, L., 2011. Decline of leaf hydraulic conductance with dehydration: relationship to leaf size and venation architecture. Plant Physiol. 156, 832–843.
Song, Y.C., 1988. The essential characteristics and main types of the broad-leaved evergreen forest in China. Phytocoenologia 16, 105–123.
Sperry, J.S., Hacke, U.G., Pittermann, J., 2006. Size and function in conifer tracheids and angiosperm vessels. Am. J. Bot. 93, 1490–1500.
Sun, Y., Hu, H., Huang, H., Vargas-Mendoza, C.F., 2014. Chloroplast diversity and population differentiation of *Castanopsis fargesii* (Fagaceae): a dominant tree species in evergreen broad-leaved forest of subtropical China. Tree Genet. Genomes 10, 1531–1539.
Team, R.Core, 2017. R: a Language and Environment for Statistical Computing. Available at:. https://www.R-project.org/.
Tyree, M.T., Davis, S.D., Cochard, H., 1994. Biophysical perspectives of xylem evolution: is there a tradeoff of hydraulic efficiency for vulnerability to dysfunction? IAWA J. 15, 335–360.
Villar-Salvador, P., Castro-Díez, P., Pérez-Rontomé, C., Montserrat-Martí, G., 1997. Stem xylem features in three *Quercus* (Fagaceae) species along a climatic gradient in NE Spain. Trees 12, 90–96.
Voelker, S.L., Noirot-Cosson, P.-E., Stambaugh, M.C., McMurry, E.R., Meinzer, F.C., Lachenbruch, B., et al., 2012. Spring temperature responses of oaks are synchronous with North Atlantic conditions during the last deglaciation. Ecol. Monogr. 82, 169–187.
Wang, P., Clemens, S., Beaufort, L., Braconnot, P., Ganssen, G., Jian, Z., et al., 2005. Evolution and variability of the Asian monsoon system: state of the art and outstanding issues. Quat. Sci. Rev. 24, 595–629.
Wang, X.-H., Kent, M., Fang, X.-F., 2007. Evergreen broad-leaved forest in Eastern China: its ecology and conservation and the importance of resprouting in forest restoration. For. Ecol. Manage. 245, 76–87.
Wheeler, J.K., Sperry, J.S., Hacke, U.G., Hoang, N., 2005. Inter-vessel pitting and cavitation in woody Rosaceae and other vesselled plants: a basis for a safety versus efficiency trade-off in xylem transport. Plant Cell Environ. 28, 800–812.
Wiens, J.J., Reeder, T.W., Oca, A.N.M.D., 1999. Molecular phylogenetics and evolution of sexual dichromatism among populations of the yarrow's spiny lizard (*Sceloporus jarrovii*). Evolution 53, 1884–1897.
Wiens, J.J., Ackerly, D.D., Allen, A.P., Anacker, B.L., Buckley, L.B., Cornell, H.V., et al., 2010. Niche conservatism as an emerging principle in ecology and conservation biology. Ecology Letters 13, 1310–1324.
Woodcock, D.W., 1989. Distribution of vessel diameter in ring-porous trees. Aliso J. Syst. Evol. Bot. 12, 287–293.
Wortemann, R., Herbette, S., Barigah, T.S., Fumanal, B., Alia, R., Ducousso, A., et al., 2011. Genotypic variability and phenotypic plasticity of cavitation resistance in *Fagus sylvatica* L. across Europe. Tree Physiol. 31, 1175–1182.
Zhang, S.-B., Cao, K.-F., Fan, Z.-X., Zhang, J.-L., 2013. Potential hydraulic efficiency in angiosperm trees increases with growth-site temperature but has no trade-off with mechanical strength. Glob. Ecol. Biogeogr. 22, 971–981.
Zhou, G., Wei, X., Wu, Y., Liu, S., Huang, Y., Yan, J., et al., 2011. Quantifying the hydrological responses to climate change in an intact forested small watershed in Southern China. Glob. Change Biol. 17, 3736–3746.
Zhou, G., Peng, C., Li, Y., Liu, S., Zhang, Q., Tang, X., et al., 2013. A climate change-induced threat to the ecological resilience of a subtropical monsoon evergreen broad-leaved forest in Southern China. Glob. Change Biol. 19, 1197–1210.
Zhu, S.-D., Chen, Y.-J., Ye, Q., He, P.-C., Liu, H., Li, R.-H., et al., 2018. Leaf turgor loss point is correlated with drought tolerance and leaf carbon economics traits. Tree Physiol. 38, 658–663.